A study of parietal-motor connectivity by intraoperative dual cortical stimulation.

Authors: Luigi Cattaneo[1], Davide Giampiccolo[1,2], Pietro Meneghelli[2], Vincenzo Tramontano[2], Francesco Sala[1,2].

Affiliations: [1]Department of Neuroscience, Biomedicine and Movement, Section of Physiology and Psychology, University of Verona, Verona. [2]Neurosurgery Unit, Neuroscience Department, Azienda Ospedaliera Universitaria Integrata, Verona, Italy

Corresponding author:

Luigi Cattaneo, MD, PhD

Institute of Neurophysiology

Dept. of Neuroscience, Biomedicine and Movement

University of Verona

Piazzale L.A. Scuro 10

37134 Verona, Italy

Fax: +39-045-8122066

E-mail: luigi.cattaneo@univr.it

Abstract – the function of the primate's posterior parietal cortex in sensorimotor transformations is well-established, though in humans its complexity is still challenging. Well-established models indicate that the posterior parietal cortex influences motor output indirectly, by means of connections to the premotor cortex, which in turn is directly connected to the motor cortex. The possibility that the posterior parietal cortex could be at the origin of direct afferents to M1 has been suggested in humans but has never been confirmed directly. In the present work we assessed during intraoperative monitoring of the corticospinal tract in brain tumour patients the existence of short-latency effects of parietal stimulation on corticospinal excitability to the upper limb. We identified several foci within the inferior parietal lobule that drove short-latency influences on cortical motor output. Active foci were distributed along the postcentral gyrus and clustered around the anterior intraparietal area and around the parietal operculum. For the first time in humans, the present data show direct evidence in favour of a distributed system of connections from the posterior parietal cortex to the ipsilateral primary motor cortex.

Introduction

The role of the posterior parietal cortex in active behaviour

The last 40 years have witnessed a radical change in our view of the parietal cortex (Mountcastle *et al.*, 1975). The posterior parietal cortex, once labelled as "associative cortex" is now well-known for receiving multimodal sensory information and integrating it into a praxic, behaviourally-committed representation of the world around us. Solid evidence in the field of neuropsychology, neuroimaging and neurostimulation indicates that the posterior parietal cortex is necessary for goal-directed behaviour. Symptoms frequently caused by lesions of the parietal lobe include deficits in sensorimotor processes, such as optic ataxia (Andersen *et al.*, 2014) or apraxia (Goldenberg, 2009). Direct stimulation of the human parietal cortex has been shown to produce movements in all body segments (Penfield and Boldrey, 1937; Balestrini *et al.*, 2015). Current evidence indicates in the human superior parietal lobule the machinery for sensorimotor transformation in spatially-oriented movements (for reviews see Culham and Valyear, 2006, Filimon, 2010 and Gallivan and Culham, 2015) controlling also some aspects of distal prehension movements (Monaco *et al.*, 2015; Cavina-Pratesi *et al.*, 2018). Visual features of objects, used to guide distal, object-directed movements are represented in humans in the anterior intraparietal region (Culham *et al.*, 2003; Frey *et al.*, 2005; Begliomini *et al.*, 2007; Grol *et al.*, 2007; Stark and Zohary, 2008; Hinkley *et al.*, 2009; Verhagen *et al.*, 2012; Orban, 2016). The role of the inferior parietal lobule in movement is less clear. Grasping-related activity in the anterior intraparietal region is found along the descending part of the precentral sulcus, up to the parietal operculum with some specialization for tool use of the more ventral areas (Orban, 2016). More ventrally, the parietal opercular region is also thought to be a site of sensorimotor integration, mainly in the somatosensory modality (Eickhoff *et al.*, 2006*b*, *a*, 2010). Summing up, imaging data in humans indicate an extended region ranging from the superior parietal lobule to the parietal operculum involved in sensorimotor processes and specialized in distinct functional aspects.

Parietal-motor pathways.

How does the motor cortex use motor-relevant information from the posterior parietal cortex? The influence of the parietal cortex on motor output is generally considered to be indirect. According to influential models, based on monkey anatomy, the parietal cortex modulates corticospinal activity in an indirect way, through the premotor cortex (Murata *et al.*, 1997; Wise *et al.*, 2002; Rizzolatti *et al.*, 2014; Kaas and Stepniewska, 2016). However, even anatomical data in monkeys are controversial in this respect. The existence of direct, monosynaptic connections from the posterior parietal cortex to the upper limb representation of the primary motor cortex has been demonstrated by several independent works (Strick and Kim, 1978; Rozzi *et al.*, 2006; Bruni *et al.*, 2018). Such data offer the anatomical bases for a possible direct pathway by which the posterior parietal cortex might control directly corticospinal output. In addition to this, it has been recently shown that the posterior parietal cortex of macaques has a direct access to spinal motor neurons by means of corticospinal axons (Rathelot *et al.*, 2017). In humans, several recent lines of evidence have suggested that the posterior parietal cortex might have a more direct influence on motor output. Non-invasive brain stimulation, i.e. transcranial magnetic stimulation (TMS) suggests that the parietal cortex could give origin to direct cortico-cortical connections to the primary motor cortex (M1) (Koch *et al.*, 2007, 2008*b*, 2010; Ziluk *et al.*, 2010; Cattaneo and Barchiesi, 2011; Karabanov *et al.*, 2013; Maule *et al.*, 2015), involved in skilled upper limb movements. Summing up, there is ample evidence in both nonhuman and human primates to support the possibility that the parietal lobe could modulate corticospinal output also directly through M1, besides the well-established indirect pathway through a relay in the premotor cortex (see Koch and Rothwell (2009) and Vesia and Davare (2011) for a review of parieto-M1 interaction models). The active role of the posterior parietal cortex in producing movements is being currently re-evaluated as a potential source of "pre-motor" afferents to the premotor cortex, where pre-motor is used here in a functional sense rather than anatomical. Imaging data provided indirect evidence of posterior parietal-motor anatomical and functional connectivity (Guye *et al.*, 2003; Koch *et al.*, 2010; Yin *et al.*, 2012). However, direct evidence in favour of direct connections between the parietal and the motor cortex in humans are lacking.

Testing direct parieto-motor pathways intraoperatively

We aim to fill this gap in current knowledge with the present work in which we tested cortico-cortical connectivity by means of intra-operative direct cortical stimulation (DCS) with a dual-pulse paradigm similar to that employed with dual-coil TMS (Koch and Rothwell, 2009). Supra-threshold test stimuli were delivered to M1 and the resulting motor evoked potentials (MEPs) were systematically recorded form distal upper limb muscles, and in some cases from facial and lower limb muscles. In some trials a conditioning stimulus was delivered to different regions of the parietal cortex at variable inter-stimulus intervals (ISIs) ranging from 4ms to 16 ms. In some other trials, only conditioning stimuli were delivered. The conditioning stimulus itself does not activate the corticospinal motor pathways, as witnessed by the systematic absence of MEPs in such trials. The modulation of motor output by conditioning stimuli is generally considered as evidence of cortico-cortical functional connectivity between the target of conditioning stimuli and the motor cortex. It is important to note that a necessary pre-requisite for the realization of dual-stimulation paradigms is that the corticospinal tract must be activated trans-synaptically by the test stimuli, because direct axonal stimulation of corticospinal axons produces MEPs that arise downstream of the putative site of interaction between the conditioning and the test stimuli. In this respect, the information currently available indicates that direct cortical stimulation (DCS) is effective also under general anaesthesia in exciting cortical output trans-synaptically, also at low stimulation intensities (Katayama *et al.*, 1988; Hanajima *et al.*, 2002; Yamamoto *et al.*, 2004; Lefaucheur *et al.*, 2010). Invasive intra-operative monitoring (IONM) in neurosurgery therefore offers the unique opportunity to assess cortico-cortical connectivity *in vivo*, with extraordinary spatial resolution and anatomical precision. Indeed, the results of the present work indicated a diffuse field of parietal spots exerting short-latency modulation of corticospinal output in the range of 6-15 ms of inter-stimulus intervals, distributed along the post-central sulcus. Such active spots showed higher density in two large clusters in the anterior intraparietal region and in the parietal operculum. We show that the anterior portion of the inferior parietal lobule and intraparietal region can be functionally considered as a “pre-motor” region. The behavioural significance of such connections is yet to be determined.

Methods

Patients

The study proposal is in accordance with ethical standards of the Declaration of Helsinki. All stimulations and recordings were performed in the context of clinical intraoperative neurophysiological monitoring (IONM). Patients scheduled for tumour removal in the vicinity of the parietal cortex were screened for enrolment. The inclusion criteria were: (1) brain tumour necessitating intraoperative neurophysiological monitoring (2) over 18 years of age. Exclusion criteria were (1) extended cortico-subcortical damage to the parietal lobe (2) voluntary decision of the patient not to be included in the cohort. Seventeen patients (age 39-79; 10M-7F; 17 right-handed) were included in this study, recruited from the Verona University Hospital. Patient’s characteristics are presented in Table 1.

Stereotaxic neuronavigation and electrode placement

MRI scans of each patient’s brain were acquired before surgery on a 3T scanner with an eight-channel head coil (Signa *3T*, *General Electric* Healthcare, Milwaukee, USA). T1-weighted 3D MPRAGE images were acquired using the following parameters (echo train length: 1, TE: 2.67ms, TR: 2.000, matrix size: 256 × 246, slice thickness: 1mm). T2-weighted, FLAIR images were also acquired (TR 6000ms, TE 150mss, TI 2000ms). The reconstruction of the individual cortical surface was performed using Brainsuite (Brainsuite, UCLA Brain Mapping Center, San Francisco, USA “Shattuck DW and Leahy RM (2002)”). For a clearer intraoperative visualization of sulcal anatomy, a skull stripped T1 using a non-uniformity correction (Brainsuite, UCLA Brain Mapping Center, San Francisco, USA “Shattuck DW and Leahy RM (2002)”) or a FLAIR images was added to the 3D visualization of the Neuronavigation system (Stealth Station 7, Medtronic, Minneapolis, USA). Correspondence of 3D reconstruction and individual patient’s sulcal anatomy was then performed using the Neuronavigation pointer. Brain anatomy was systematically analysed prior to surgery so that main sulcal patterns of the postcentral and parietal region could be readily identified during actual surgery. The stimulating strip was placed parallel to the

central sulcus, similarly to the montage used for studies of intra-operative motor evoked potentials, after identification of the central sulcus by phase reversal (Romstöck *et al.*, 2002). Placement of the conditioning electrode strip was roughly planned a priori but was systematically reprogrammed when in presence of contingent surgical conditions preventing the placement of the strip in the desired position, such as presence of large vessels or space requirements by the ongoing surgical procedures.

Anaesthesia and conventional IONM

The anaesthesia protocol applied was Total Intravenous Anaesthesia (TIVA). More precisely, a continuous infusion of Propofol (100-150 µg/kg/min) and Fentanyl (1µg/kg/min) was used, avoiding bolus. Short acting relaxants were administered for intubation purpose only and then avoided. Halogenated anaesthetic agents were never used. Since all patients were candidates for IONM of the corticospinal tract, standard neurophysiological monitoring and mapping was performed. This involved simultaneous acquisition of continuous electroencephalography (EEG), electrocorticography (ECoG), recording of free-running electromyographic (EMG) activity (ISIS-IOM, Inomed Medizintechnik GmbH, Emmendingen, Germany). Muscle MEPs were initially elicited by Transcranial Electrical Stimulation (TES) via corkscrew-like electrodes (Ambu® Neuroline Corkscrew, Ambu, Copenhagen, Denmark) from the scalp. Short trains of 5 square-wave stimuli of 0.5 ms duration, and interstimulus interval (ISI) of 4ms were applied at a repetition rate up to 2 Hz through electrodes placed at C1 and C2 scalp sites, according to the 10/20 EEG system. Cortical and subcortical stimulation were performed using a monopolar probe (45 mm, angled 30°, Inomed Medizintechnik GmbH, Emmendingen, Germany) referenced to Fz. Stimulation parameters were as follows: a short train of five pulses, pulse duration 0.5 milliseconds; interstimulus interval (ISI) 2 ms at 1 Hz repetition rate. Cortical stimulation was anodal while subcortical stimulation was cathodal. Once the dura was opened, MEP monitoring was performed using a 6-contacts strip electrode (diameter 2.5 mm, space 10 mm, contact strips: 0.7 mm thin, 10 mm width, Inomed Medizintechnik GmbH, Emmendingen, Germany). EMG recordings were performed in a belly-tendon montage, by means of subcutaneous needle monopolar electrodes (Ambu® Neuroline Subdermal, Ambu, Copenhagen, Denmark). The *orbicularis oris*, the ABP, the *biceps*, the *abductor hallucis* and the *tibialis anterior* muscles contralateral to the stimulated hemisphere were recorded.

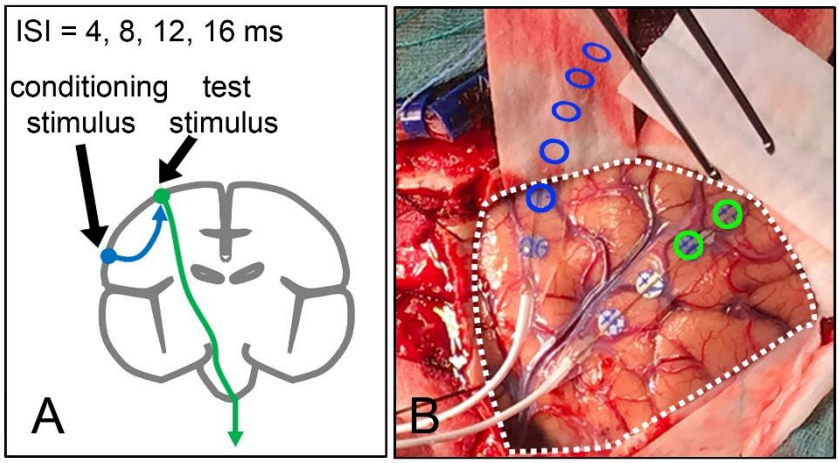

Figure 1: A- *schematic representation of the dual strip protocol. Test stimuli are delivered to the motor cortex and produce a measurable motor evoked potential via the corticospinal tract (green arrow). In some trials the test stimulus is preceded by a conditioning stimulus, which alone cannot activate the corticospinal tract, applied to the parietal cortex (blue arrow). The inter-stimulus interval (ISI) ranges between 4 and 16 ms. The finding of MEPs to conditioning stimuli having a different amplitude or area than MEPs to test stimuli alone is considered evidence for functional connectivity between the two stimulated regions. The short duration of the ISI, in the range of milliseconds, indicates mono-or oligo-synaptic connections.* ***B-*** *Actual surgical scenario (patient #4). The dashed white line represents the borders of the craniotomy. The two stimulation strips are shown. The test stimulus dipole is indicated with the two green circles and is used to activate the corticospinal tract. The*

conditioning strip is placed over the parietal lobe. The dipoles used for conditioning stimuli are indicated with blue circles. Note that the electrode strip is inserted under the dura, therefore the electrode position extends well beyond the craniotomy.

Dual strip stimulation

Direct electrical cortical stimulation was applied to the precentral gyrus (test stimuli) via a 6-contacts strip electrode and to the parietal cortex by means of a 6-contacts or an 8-contacts strip electrode (Figure 1 shows a schematic of the dual strip protocol and an example of surgical scenario). To optimize timing precision between the conditioning and the test stimuli, the conditioning stimuli were always delivered in a short train of 2 stimuli at 250 Hz and of 0.5 ms duration. Test stimuli were delivered with trains of the minimal duration required to elicit a stable MEP in the ABP. This results in test stimulation with one single stimulus in 1 patient, with 2 stimuli in 12 patients and with 3 stimuli in 3 patients. Intensity of test stimulation was set to obtain a MEP from the thenar muscle of around 500 uV peak-peak amplitude. The ISI was considered as the interval between the last stimulus of the conditioning train and the last pulse of the test train. The ISIs of 7, 13 and 18 ms were systematically explored in separate blocks for each of the test-stimulus electrodes. Every block contained at least 15 repetitions of the same dual stimulation. Dual-stimulation blocks were alternated with blocks with only test-stimuli so that the unconditioned MEP amplitude was monitored throughout the recording session. The timing of dual stimuli was manged entirely by the commercially available ISIS-IOM system (Inomed Medizintechnik GmbH, Emmendingen, Germany) by means of the "facilitation" function, that allows independent electrical stimulation through two separate output channels.

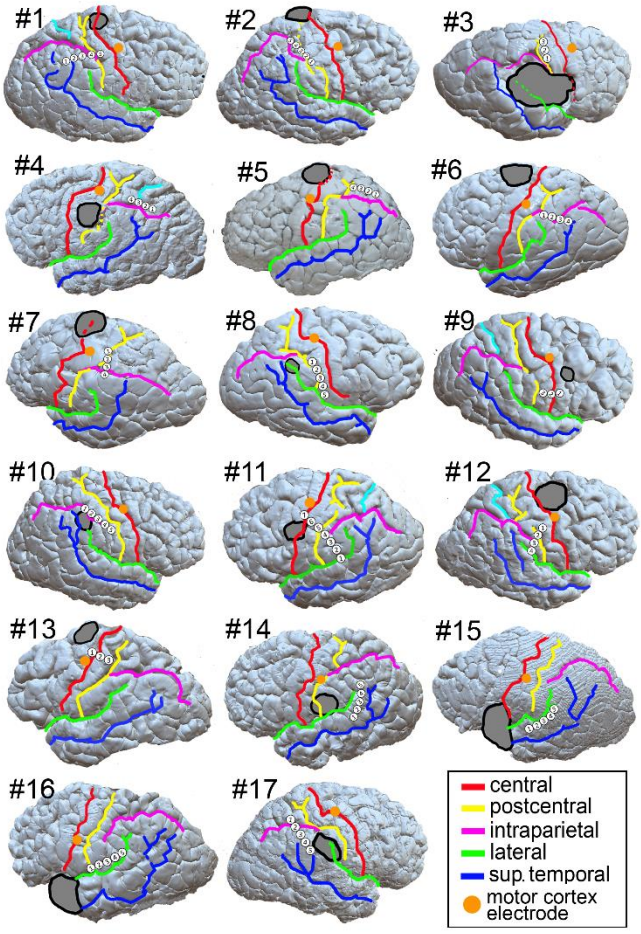

Figure 2: *rendering of the individual brains (only the stimulated hemisphere is shown. The projection of the lesion on the surface is indicated with the grey shape. Main cortical sulci are indicated with a colour code as indicated in the legend. The orange spot indicates the point of corticospinal stimulation (test stimulus). The*

white numbered circles indicate the position of the cathode of conditioning stimulation. (note that conditioning stimuli have been delivered in bipolar modality).

Data analysis

Pre-processing required the data to be exported in digital format and analysed with the MATLAB software. The EMG traces were band-pass filtered (50-2000 Hz) and rectified. The duration of the MEP was determined individually, and the corresponding area of the EMG recording was extracted. In this way each trial was characterized by a single number, i.e. the MEP area. We then proceeded to normalizing conditioned MEPs to test MEPs. However, MEPs to test stimuli alone are not stable throughout the surgical procedure because of strip movements. To correct for such variability, we normalized blocks of conditioned MEPs only to a sliding window of the blocks of test stimuli adjacent to each conditioned block. This was done by dividing the single conditioned MEP areas by the median of the test MEP areas. The resulting normalized conditioned MEP areas (normMEP) were used as main experimental variable. The main analysis was carried out in single patients, comparing normalized conditioned MEP areas from test stimuli by means of independent-samples t-tests. This test informs us whether, in single subjects, the trials in a given conditioned set are different from those in the test set and the direction of the change (excitation or inhibition). Significance threshold was corrected to account for the repeated comparisons. Analysis were performed therefore on single subjects, using a univariate approach. The results of single t-tests were therefore corrected for multiple comparisons in each participant. For example, patient #1 was tested on 20 cortical spots and therefore critical p-value was set to p=0.05/20 i.e. p=0.0025. Qualitative assessment of the effects of conditioning stimuli at the population level was performed by plotting on a standardized surface map of the parietal cortex the sites of conditioning stimulation of all participants, indicating electrodes that had a significant effect on test stimuli in single participants. To this purpose, we used the frameless stereotaxic neuronavigation system to pinpoint ion individual brain anatomies the real position of strip electrodes and the trajectory of strips that were not readily visible because in the subdural space. The parietal region shows a considerable inter-individual variability, therefore, to remap individual anatomies on the standardized space we made reference to the anatomical study of Zlatkina and Petrides (2014), which resulted in slight warping of the strip positions. Figure 2 indicates individual brain anatomies of the 16 patients together with the conditioning strip electrodes and Figure 3 Indicates the population data in the standardized space.

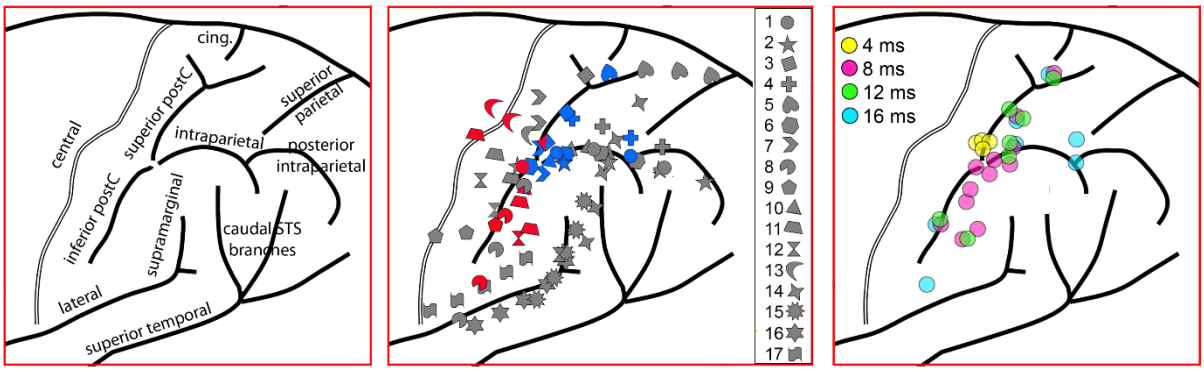

Figure 3: *standardized parietal anatomy showing the location of each participant's conditioning electrodes in the parietal cortex. The anatomical template is based on (Zlatkina and Petrides, 2014; Zlatkina et al., 2016). The* ***left panel*** *shows the label of the main sulci. The* ***middle panel*** *indicates the positions of conditioning stimuli (cathodes) in each patient. The legend links symbols to each patient's numbers. Grey-filled symbols indicate spots with no significant effect. Blue-filled symbols indicate spots with significant inhibitory conditioning effects. Red-filled symbols indicate spots with significant excitatory conditioning effects. Spots in which both excitatory and inhibitory effects were observed at different ISIs are indicated with both red and blue filling. The* ***right panel*** *shows only conditioning spots with significant effects (active spots), pooled across patients and grouped according to the ISI at which an effect was observed.*

Results

In all participants it was possible to stimulate at least one conditioning spot, with a variable number of 3-6. Figure 2 shows each patient's anatomy together with lesion location and electrode placement. For the sake of clarity, participants have been numbered according to the presence of excitatory effect, inhibitory effects or no effect. We observed in most subjects a significant modulation of MEPs by conditioning stimuli in one specific electrode, at specific timings. The individual results are reported in Figures 3 and 4 and in Table 2. We observed both inhibitory and excitatory effects of conditioning stimuli at different ISIs. The systematic between-subject variations inherent in the mapping technique were reflected in the variability of the ISIs at which conditioning stimuli exerted a significant effect on corticospinal excitability which ranged from 4ms to 16 ms. 6 participants showed only inhibitory effects, 3 showed mixed effects, 4 showed faciliatory effects and 4 did not show any effect of conditioning stimuli on corticospinal excitability.

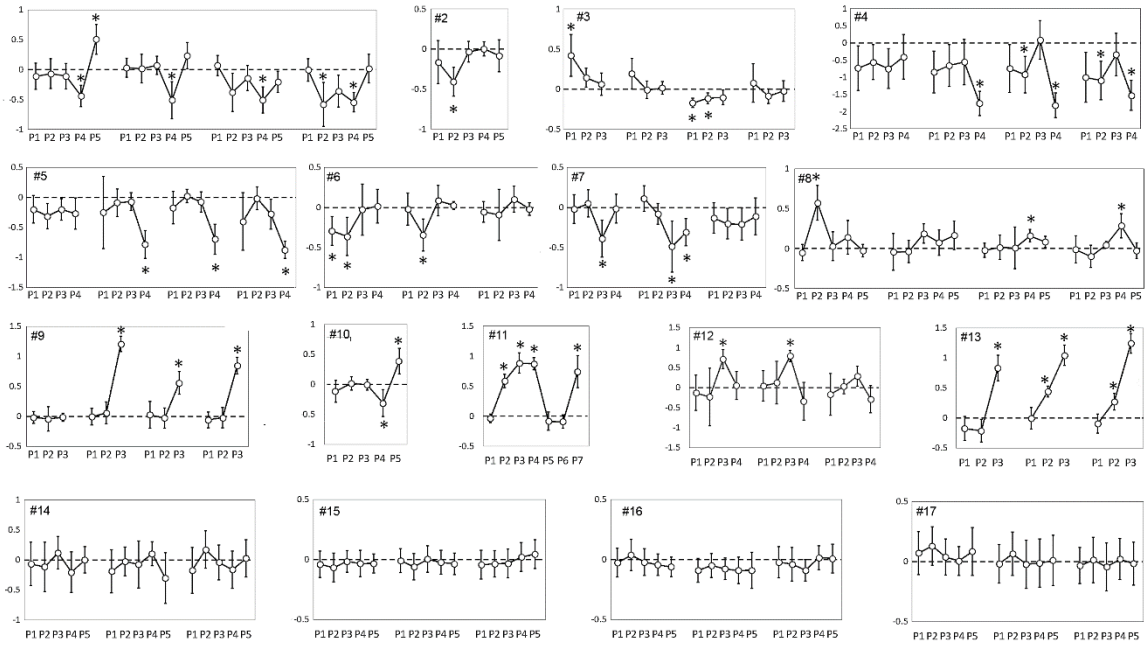

Figure 4. *Comprehensive data from all patients. The plots indicate the mean value of the log-transformed ratios between conditioned and unconditioned MEPs. Negative values indicate that the mean conditioned MEP is smaller than the mean test MEP (inhibitory effects). Positive values indicate that mean conditioned MEPs are larger than mean test MEPs (excitatory effects). All log-ratios have been tested by single-sample t-tests against a null hypothesis of mean value = 0. Significance threshold was Bonferroni corrected. Asterisks indicate significant comparisons. Error bars indicate 95% confidence intervals of the mean).*

Anatomical localization and chronometry of conditioning stimulus effects

Each patient was stimulated with conditioning stimuli in 2-5 pairs of stimulating electrodes (Figure 2 indicates the cathode of the bipolar stimulation montages). Active spots were localized all along a region of the PPC immediately posterior to the post-central sulcus (Figure 3 – middle panel). In addition, in the few participants in which the conditioning stimulus strip reached the central sulcus, we observed a small cluster of active spots corresponding to the hand motor cortex. We did not observe significant effects from stimulation of the post-central gyrus at the ISIs adopted here. The polarity of the effect was spatially organized. We observed inhibitory effects of conditioning stimuli applied to the superior parietal lobule and the anterior intraparietal region. We found excitatory effects from conditioning stimuli applied to the inferior parietal lobule. Most patients showed only facilitatory or inhibitory effects in all stimulation dipoles. In two patients (#1 and #10) we observed a change in polarity of the effect from inhibitory to facilitatory moving the stimulating electrode

ventrally and rostrally. All spots showed the same polarity of effect, whenever present, at all ISIs, with the sole exception of a single spot in a single patient (#3), localized in the intraparietal region, that showed facilitatory effects at the 4ms ISI and inhibitory effects at the 12 ms ISI. Figure 3 – right panel, shows the anatomical localization of effective conditioning stimuli, grouped by ISI. The spots with effects at 4 ms were all clustered in proximity of the hand motor area, while effective spots at higher ISIs increased gradually their distance from hand-M1.

Discussion

Three distinct regions in the parietal cortex exert specific short-latency effects on upper-limb corticospinal excitability.

In the present work we demonstrate for the first time the existence of direct parietal-motor functional connections in humans by means of direct cortical stimulation. The presence of short-latency modulations of conditioning stimuli implies that the two regions are functionally connected. (Koch and Rothwell, 2009). We identified several cortical spots in the posterior parietal cortex that exert a short-latency effect on the excitability of the corticospinal pathway to the upper limb. Combining spatial distribution and polarity (excitatory or inhibitory) of the conditioning effects, we identified three distinct regions: a ventral region, corresponding to the part of the supramarginal gyrus immediately posterior to the inferior postcentral sulcus, extending ventrally to the parietal opercular region, a dorsal inhibitory region comprising the junction between the intraparietal sulcus and the precentral sulcus and the portion of the superior parietal lobule adjacent to the postcentral sulcus. A third region was indicated by a small cluster of 2 electrodes along the intraparietal sulcus, around its middle portion. However, we should consider that the spatial sampling procedure employed here suffers from a main limitation, that is, conditioning stimuli have been delivered on the crown of the sulci, because the surgical procedures do not imply the opening of the arachnoid and widening of the sulci. As such, our map of the parietal cortex is patchy and strongly biased towards the crown of the gyri.

Widespread representation of upper limb movements in the posterior parietal cortex.

In our study we focussed on the motor representation of the distal upper limb. A striking result is that the posterior parietal cortex seems to contain a widespread representation of the upper limb. Having tested only one effector, we cannot draw any conclusions on somatotopy, but our partial results argue against a possible somatotopic arrangement of motor representations in the PPC, in opposition of what we could have expected in the premotor region where rough somatotopy is suggested by several studies (Cunningham *et al.*, 2013). Conversely, the posterior parietal cortex, albeit embedded with consistent motor representations, has not been shown to be organized effector-wise in humans. Action representations in the PPC of humans seem to show an upper limb preference and a spatial organization that reflects the type of action rather than the effector used, except for eye movements that are supported by a specialized network (Grefkes and Fink, 2005). Most authors seem to agree on a motor map of the rostral PPC organized in a medial-lateral system. Spatially-oriented stimuli are coded in the SPL, object-directed movements in the mid-portion, corresponding to the intraparietal sulcus and more complex hand actions such as symbolic movements and tool use are coded in the IPL (Gallivan and Culham, 2015; Orban, 2016). Consequently, the finding of hand representations throughout its medio-lateral extension is supported by current knowledge on the physiology of motor properties of the human PPC.

A direct parieto-motor pathway in humans.

Neuroimaging studies in humans however, are not able to specify the actual neural pathways by which the PPC can modulate movement. The novelty of the present study is providing compelling evidence that one possible neural substrate of the PPC influence on action is fast, probably direct, parieto-motor connectivity. The temporal characteristics of the parieto-motor interactions are illustrated in Figure 3C. We show a general pattern of active spots modulating the output of hand-M1 at ISIs that are roughly proportional to the distance between the active spot and M1, compatibly with axonal conduction of action potentials. Active spots that exert modulation at 4 ms ISIs are all clustered nearby the hand-M1. Active spots that are effective at longer ISIs

are located progressively further away from the hand-M1. The two spots in the mid-intraparietal cluster both appeared at 16 ms. This pattern indicates that effective ISIs scale positively with linear distance to hand-M1. There are two main inferences to be made from this finding: First, that the effect on conditioning stimuli on the PPC is not likely to be due to current spread to M1, because current spread is *quasi*-instantaneous, and the latency of its effect would not increase with distance. Second, the increasing latency of the conditioning effects with increasing distance from M1 argues against the possibility that the site of interaction between parietal output and the corticospinal pathway is subcortical or spinal because in that case we would expect similar latencies of conditioning effects. On the contrary, the pattern of co-variation of distance to hand-M1 with effective ISI is strongly in favour of cortico-cortical connections between PPC and hand-M1 mediating the conditioning effect.

Effects of anaesthesia

All our patients have been tested under the TIVA protocol. The main effect of propofol is a strong enhancement of GABAergic inputs (Franks, 2008). In terms of brain connectivity, Propofol dampens extensive cortico-cortical connections, according to TMS-EEG studies (Sarasso et al., 2015). The strength of oligosynaptic pathways is affected but generally not to the level of a conduction block, as witnessed by the validity of somatosensory evoked potentials and motor evoked potentials, which are mediated by multi-synaptic neural chains. The TIVA protocol is titrable, and it was systematically kept at low levels of neural suppression (see methods). Therefore, the anaesthesiologic setting employed here is appropriate to test mono- or oligo-synaptic connections, though we cannot make any inference on how these connections would work in the awake state. Summing up, the implications of testing cortico-cortical connectivity under anaesthesia are that: A) significant effects can be considered as genuine expression of oligo-synaptic connections, B) non-significant stimulations could underlie either no connections or multi-synaptic connections which are dampened by anaesthesia and C) we cannot make any inference on how the highlighted connections would function in the awake state and even more so during active tasks.

Relation to connectivity data obtained with non-invasive brain stimulation

Ipsilateral PPC-M1 connections have been tested non-invasively by dual-coil TMS in awake subjects in a series of studies (Koch *et al.*, 2007, 2008*b*, *a*, 2010; Koch and Rothwell, 2009; Ziluk *et al.*, 2010; Cattaneo and Barchiesi, 2011; Vesia and Davare, 2011; Karabanov *et al.*, 2012, 2013; Vesia *et al.*, 2013, 2017; Chao *et al.*, 2015; Maule *et al.*, 2015). The present results cannot be compared to these studies in alert subjects in terms of polarity (inhibition or excitation) nor of task-dependency of the response because of the anaesthesia, but they can be compared in terms of cortical site in the PPC and timing of conditioning stimuli that exert a significant effect onto M1. Our data are compatible with the findings of Karabanov *et al.* (2013) showing two foci along the intraparietal sulcus, the two clusters of active spots along the intraparietal sulcus in the present findings (Figure 3B). The cluster of spots active at 4 ms ISI (Figure 3C) shows striking similarities with the findings of Vesia *et al.* (2013). The most ventral spots along the postcentral sulcus are in the same location as the opercular region that was stimulated in Maule *et al.* (2015). The posterior intraparietal spot stimulated in Koch *et al.* (2007, 2008*b*) is similar or slightly posterior to the posterior cluster of active spots observed here. Summing up, the current systematic mapping of the PPC is consistent with most of the previous data testing single cortical spots with non-invasive brain stimulation.

Summary

We show conclusive evidence that in humans direct parieto-motor pathways exist. We investigated motor output to the distal upper limb and found a widespread representation of the hand with seemingly no specific spatial distribution that could parallel the somatotopy of the adjacent somatosensory cortex. Such absence of topographic distribution is well supported by previous data in non-human and human primates that indicate a spatial organization of motor features in the PPC reflecting action types rather than effectors. We did find a specific spatial clustering of motor spots in the PPC according to the polarity of the effect on corticospinal output and to spatial location. A ventral cluster showed excitatory effects, while a dorsal cluster showed inhibitory effects. A third cluster was identified due to its localization, in the mid-portion of the intraparietal

sulcus. The clinical neurosurgeon's attention toward motor function of the parietal lobe is increasingly recognized (Rossi *et al.*, 2018). The present data are potentially exploitable as an IONM procedure for the monitoring of complex motor functions, though further investigations are required.

REFERENCES

Andersen RA, Andersen KN, Hwang EJ, Hauschild M. Optic ataxia: From balint's syndrome to the parietal reach region. Neuron 2014; 81: 967–983.

Balestrini S, Francione S, Mai R, Castana L, Casaceli G, Marino D, et al. Multimodal responses induced by cortical stimulation of the parietal lobe: A stereo-electroencephalography study. Brain 2015; 138: 2596–2607.

Begliomini C, Wall MB, Smith AT, Castiello U. Differential cortical activity for precision and whole-hand visually guided grasping in humans. Eur J Neurosci 2007; 25: 1245–1252.

Bruni S, Gerbella M, Bonini L, Borra E, Coudé G, Ferrari PF, et al. Cortical and subcortical connections of parietal and premotor nodes of the monkey hand mirror neuron network. Brain Struct Funct 2018; 223: 1713–1729.

Cattaneo L, Barchiesi G. Transcranial magnetic mapping of the short-latency modulations of corticospinal activity from the ipsilateral hemisphere during rest. Front Neural Circuits 2011; 5

Cavina-Pratesi C, Connolly JD, Monaco S, Figley TD, Milner AD, Schenk T, et al. Human neuroimaging reveals the subcomponents of grasping, reaching and pointing actions. Cortex 2018; 98: 128–148.

Chao CC, Karabanov AN, Paine R, Carolina De Campos A, Kukke SN, Wu T, et al. Induction of motor associative plasticity in the posterior parietal cortex-primary motor network. Cereb Cortex 2015; 25: 365–373.

Culham JC, Danckert SL, DeSouza JFX, Gati JS, Menon RS, Goodale MA. Visually guided grasping produces fMRI activation in dorsal but not ventral stream brain areas. Exp Brain Res 2003; 153: 180–189.

Culham JC, Valyear KF. Human parietal cortex in action. Curr Opin Neurobiol 2006; 16: 205–212.

Cunningham DA, Machado A, Yue GH, Carey JR, Plow EB. Functional somatotopy revealed across multiple cortical regions using a model of complex motor task. Brain Res 2013; 1531: 25–36.

Eickhoff SB, Amunts K, Mohlberg H, Zilles K. The human parietal operculum. II. Stereotaxic maps and correlation with functional imaging results. Cereb Cortex 2006; 16: 268–279.

Eickhoff SB, Jbabdi S, Caspers S, Laird a. R, Fox PT, Zilles K, et al. Anatomical and Functional Connectivity of Cytoarchitectonic Areas within the Human Parietal Operculum. J Neurosci 2010; 30: 6409–6421.

Eickhoff SB, Schleicher A, Zilles K, Amunts K. The human parietal operculum. I. Cytoarchitectonic mapping of subdivisions. Cereb Cortex 2006; 16: 254–267.

Filimon F. Human cortical control of hand movements: parietofrontal networks for reaching, grasping, and pointing. Neuroscientist 2010; 16: 388–407.

Franks NP. General anaesthesia: From molecular targets to neuronal pathways of sleep and arousal. Nat Rev Neurosci 2008; 9: 370–386.

Frey SH, Vinton D, Norlund R, Grafton ST. Cortical topography of human anterior intraparietal cortex active during visually guided grasping. Cogn Brain Res 2005; 23: 397–405.

Gallivan JP, Culham JC. Neural coding within human brain areas involved in actions. Curr Opin Neurobiol 2015; 33: 141–149.

385 Goldenberg G. Apraxia and the parietal lobes. Neuropsychologia 2009; 47: 1449–1459.

386 Grefkes C, Fink GR. The functional organization of the intraparietal sulcus in humans and monkeys. J Anat 2005;
387 207: 3–17.

388 Grol MJ, Majdandzic J, Stephan KE, Verhagen L, Dijkerman HC, Bekkering H, et al. Parieto-Frontal Connectivity
389 during Visually Guided Grasping. J Neurosci 2007; 27: 11877–11887.

390 Guye M, Parker GJ., Symms M, Boulby P, Wheeler-Kingshott CA., Salek-Haddadi A, et al. Combined functional
391 MRI and tractography to demonstrate the connectivity of the human primary motor cortex in vivo. Neuroimage
392 2003; 19: 1349–1360.

393 Hanajima R, Ashby P, Lang AE, Lozano AM. Effects of acute stimulation through contacts placed on the motor
394 cortex for chronic stimulation. Clin Neurophysiol 2002; 113: 635–641.

395 Hinkley LBN, Krubitzer LA, Padberg J, Disbrow EA. Visual-Manual Exploration and Posterior Parietal Cortex in
396 Humans. J Neurophysiol 2009; 102: 3433–3446.

397 Kaas JH, Stepniewska I. Evolution of posterior parietal cortex and parietal-frontal networks for specific actions
398 in primates. J Comp Neurol 2016; 524: 595–608.

399 Karabanov A, Jin S-H, Joutsen A, Poston B, Aizen J, Ellenstein A, et al. Timing-dependent modulation of the
400 posterior parietal cortex-primary motor cortex pathway by sensorimotor training. J Neurophysiol 2012; 107:
401 3190–3199.

402 Karabanov AN, Chao CC, Paine R, Hallett M. Mapping different intra-hemispheric parietal-motor networks using
403 twin coil TMS. Brain Stimul 2013; 6: 384–389.

404 Katayama Y, Tsubokawa T, Maejima S, Hirayama T, Yamamoto T. Corticospinal direct response in humans:
405 Identification of the motor cortex during intracranial surgery under general anaesthesia. J Neurol Neurosurg
406 Psychiatry 1988; 51: 50–59.

407 Koch G, Cercignani M, Pecchioli C, Versace V, Oliveri M, Caltagirone C, et al. In vivo definition of parieto-motor
408 connections involved in planning of grasping movements. Neuroimage 2010; 51: 300–312.

409 Koch G, Fernandez Del Olmo M, Cheeran B, Ruge D, Schippling S, Caltagirone C, et al. Focal Stimulation of the
410 Posterior Parietal Cortex Increases the Excitability of the Ipsilateral Motor Cortex. J Neurosci 2007; 27: 6815–
411 6822.

412 Koch G, Oliveri M, Cheeran B, Ruge D, Gerfo E Lo, Salerno S, et al. Hyperexcitability of parietal-motor functional
413 connections in the intact left-hemisphere of patients with neglect. Brain 2008; 131: 3147–3155.

414 Koch G, Del Olmo MF, Cheeran B, Schippling S, Caltagirone C, Driver J, et al. Functional Interplay between
415 Posterior Parietal and Ipsilateral Motor Cortex Revealed by Twin-Coil Transcranial Magnetic Stimulation during
416 Reach Planning toward Contralateral Space. J Neurosci 2008; 28: 5944–5953.

417 Koch G, Rothwell JC. TMS investigations into the task-dependent functional interplay between human posterior
418 parietal and motor cortex. Behav Brain Res 2009; 202: 147–152.

419 Lefaucheur JP, Holsheimer J, Goujon C, Keravel Y, Nguyen JP. Descending volleys generated by efficacious
420 epidural motor cortex stimulation in patients with chronic neuropathic pain. Exp Neurol 2010; 223: 609–614.

421 Maule F, Barchiesi G, Brochier T, Cattaneo L. Haptic working memory for grasping: The role of the parietal
422 operculum. Cereb Cortex 2015; 25: 528–537.

423 Monaco S, Sedda A, Cavina-Pratesi C, Culham JC. Neural correlates of object size and object location during
424 grasping actions. Eur J Neurosci 2015; 41: 454–465.

425 Mountcastle VB, Lynch JC, Georgopoulos AP, Sakata H, Acuna C. Posterior parietal association cortex of the
426 monkey: command functions for operations within extrapersonal space. J Neurophysiol 1975; 38: 871–908.

427 Murata A, Fadiga L, Fogassi L, Gallese V, Raos V, Rizzolatti G. Object representation in the ventral premotor
428 cortex (area F5) of the monkey. J Neurophysiol 1997; 78: 2226–2230.

429 Orban GA. Functional definitions of parietal areas in human and non-human primates. Proc R Soc B Biol Sci
430 2016; 283: 20160118.

431 Penfield W, Boldrey E. Somatic motor and sensory representation in the cerebral cortex of man as studied by
432 electrical stimulation. Brain 1937; 60: 389–443.

433 Rathelot J-A, Dum RP, Strick PL. Posterior parietal cortex contains a command apparatus for hand movements.
434 Proc Natl Acad Sci 2017; 114: 4255–4260.

435 Rizzolatti G, Cattaneo L, Fabbri-Destro M, Rozzi S. Cortical mechanisms underlying the organization of goal-
436 directed actions and mirror neuron-based action understanding. Physiol Rev 2014; 94: 655–706.

437 Romstöck J, Fahlbusch R, Ganslandt O, Nimsky C, Strauss C. Localisation of the sensorimotor cortex during
438 surgery for brain tumours: Feasibility and waveform patterns of somatosensory evoked potentials. J Neurol
439 Neurosurg Psychiatry 2002; 72: 221–229.

440 Rossi M, Fornia L, Puglisi G, Leonetti A, Zuccon G, Fava E, et al. Assessment of the praxis circuit in glioma
441 surgery to reduce the incidence of postoperative and long-term apraxia: a new intraoperative test. J Neurosurg
442 2018; 130: 1–11.

443 Rozzi S, Calzavara R, Belmalih A, Borra E, Gregoriou GG, Matelli M, et al. Cortical connections of the inferior
444 parietal cortical convexity of the macaque monkey. Cereb Cortex 2006; 16: 1389–1417.

445 Sarasso S, Boly M, Napolitani M, Gosseries O, Charland-Verville V, Casarotto S, et al. Consciousness and
446 complexity during unresponsiveness induced by propofol, xenon, and ketamine. Curr Biol 2015; 25: 3099–3105.

447 Stark A, Zohary E. Parietal mapping of visuomotor transformations during human tool grasping. Cereb Cortex
448 2008; 18: 2358–2368.

449 Strick PL, Kim CC. Input to primate motor cortex from posterior parietal cortex (area 5). I. Demonstration by
450 retrograde transport. Brain Res 1978; 157: 325–330.

451 Verhagen L, Dijkerman HC, Medendorp WP, Toni I. Cortical Dynamics of Sensorimotor Integration during Grasp
452 Planning. J Neurosci 2012; 32: 4508–4519.

453 Vesia M, Barnett-Cowan M, Elahi B, Jegatheeswaran G, Isayama R, Neva JL, et al. Human dorsomedial parieto-
454 motor circuit specifies grasp during the planning of goal-directed hand actions. Cortex 2017; 92: 175–186.

455 Vesia M, Bolton DA, Mochizuki G, Staines WR. Human parietal and primary motor cortical interactions are
456 selectively modulated during the transport and grip formation of goal-directed hand actions. Neuropsychologia
457 2013; 51: 410–417.

458 Vesia M, Davare M. Decoding Action Intentions in Parietofrontal Circuits. J Neurosci 2011; 31: 16491–16493.

459 Wise SP, Boussaoud D, Johnson PB, Caminiti R. Premotor and Parietal Cortex: Corticocortical Connectivity and
460 Combinatorial Computations. Annu Rev Neurosci 2002; 20: 25–42.

461 Yamamoto T, Katayama Y, Nagaoka T, Kobayashi K, Fukaya C. Intraoperative Monitoring of the Corticospinal
462 MotorEvoked Potential (D-wave): Clinical Index for PostoperativeMotor Function and Functional Recovery.
463 Neurol Med Chir 2004; 44: 170–182.

464 Yin X, Zhao L, Xu J, Evans AC, Fan L, Ge H, et al. Anatomical Substrates of the Alerting, Orienting and Executive
465 Control Components of Attention: Focus on the Posterior Parietal Lobe. PLoS One 2012; 7: e50590.

466 Ziluk A, Premji A, Nelson AJ. Functional connectivity from area 5 to primary motor cortex via paired-pulse
467 transcranial magnetic stimulation. Neurosci Lett 2010; 484: 81–85.

468 Zlatkina V, Amiez C, Petrides M. The postcentral sulcal complex and the transverse postcentral sulcus and their
469 relation to sensorimotor functional organization. Eur J Neurosci 2016; 43: 1268–1283.

470 Zlatkina V, Petrides M. Morphological patterns of the intraparietal sulcus and the anterior intermediate parietal
471 sulcus of Jensen in the human brain. Proc R Soc B Biol Sci 2014; 281: 20141493–20141493.

472

Patient #, age, dexterity, sex.	**Symptoms at presentation**	**Anatomical location of the lesion**	**Characterization of the neoplastic lesion**
#1 - 60 y-o right-handed female	Apraxia, gait disturbances, dysesthesia and weakness on the right side	Right post-central,inhomogeneous lesion	Glioma IV (WHO 2016, IDH-WT, MGMT+)
#2 - 71 y-o, right-handed male	Gait ataxia, dysarthria	Right frontal homogeneous lesion	Meningioma I (WHO 2016, A)
#3 - 62 y-o right-handed female	Left facial palsy of central type	right post-Rolandic inhomogeneous lesion	Glioma IV (WHO 2016, IDH- WT, MGMT+)
#4 - 71 y-o, right-handed male	dysesthesia and weakness of the right arm and face; mild language deficits	left anterior intraparietal inhomogeneous lesion	Metastatic melanoma (VBRAF+)
#5 - 62 y-o right-handed female	Leg weakness	Left pre-Rolandic inhomogeneous lesion	Metastatic lung adenocarcinoma (PDL-2 +)
#6 - 62 y-o right handed female	Headache	Left frontal parasagittal homogenous lesion	Meningioma I (WHO 2016, A)
#7 - 74 y-o, right-handed male	Right leg weakness	Left frontal parasagittal homogenous lesion	Meningioma II (WHO 2016, A)
#8 - 75 y-o right-handed female	Generalized seizures	Right parieto-temporal inhomogeneous lesion	Glioma IV (WHO 2016, IDH- WT, MGMT-)
#9 - 60 y-o right-handed female	Mood change	Right pre-Rolandic inhomogeneous lesion	Metastatic lung adenocarcinoma (PDL-1 +)
#10 - 67 y-o, right-handed male	Dizziness, gait ataxia	Right parieto-temporal inhomogeneous lesion	Glioma IV (WHO 2016, IDH- WT, MGMT+)
#11 - 77 y-o, right-handed male	Focal seizures, dizziness, left homonymous hemianopia	Right parieto-temporal inhomogeneous lesion	Glioma IV (WHO 2016, IDH- WT, MGMT+)
#12 - 79 y-o right handed male	Dizziness	Right Rolandic homogenous lesion	Meningioma I (WHO 2016, A-B)
#13 - 74 y-o, right-handed male	Enhancing lesion on follow up (redo)	Left superior frontal inhomogeneous lesion	Glioma IV (WHO 2016, IDH-1, MGMT+)
#14 - 32 y-o, right-handed male	Focal seizures	Right superior temporal homogenous lesion	Ganglioglioma I (WHO 2016, A-B)
#15 - 37 y-o, right-handed male	Focal seizures, mild language deficits (Redo)	Left temporal inhomogenous lesion	Glioma IV (WHO 2016, IDH- WT, MGMT-)
#16 - 49 y-o right-handed female	Generalized seizures (Redo)	Left temporo-polar inhomogeneous lesion	Glioma IV (WHO 2016, IDH- WT, MGMT+)
#17 - 52 y-o, right-handed male	Right side weakness, mild language deficits	Left temporo-polar inhomogeneous lesion	Glioma IV (WHO 2016, IDH- WT, MGMT+)

473 ***Table 1*: Demographic information on the group of patients**

474

475

patient	ISI:	conditioning stimulus cathode				
		P1	**P2**	**P3**	**P4**	**P5**
#1	4ms	-0.113 (sd: 0.22) t(19)=-1.17 p=0.2582	-0.069 (sd: 0.25) t(19)=-0.63 p=0.5378	-0.112 (sd: 0.21) t(19)=-1.18 p=0.2544	**-0.441 (sd: 0.18)** **t(19)=-5.62** **p<0.00001**	**0.508 (sd: 0.25)** **t(19)=4.59** **p=0.0002**
	8ms	0.03 (sd: 0.16) t(19)=0.42 p=0.6856	0.016 (sd: 0.24) t(19)=0.15 p=0.8814	0.071 (sd: 0.15) t(19)=1.08 p=0.2949	**-0.513 (sd: 0.31)** **t(19)=-3.69** **p=0.0016**	0.232 (sd: 0.22) t(19)=2.36 p=0.0288
	12ms	0.068 (sd: 0.17) t(19)=0.92 p=0.3688	-0.38 (sd: 0.32) t(19)=-2.66 p=0.0156	-0.143 (sd: 0.21) t(19)=-1.54 p=0.1407	**-0.511 (sd: 0.22)** **t(19)=-5.16** **p=0.0001**	-0.209 (sd: 0.18) t(19)=-2.53 p=0.0201
	16ms	-0.005 (sd: 0.19) t(19)=-0.06 p=0.9584	**-0.585 (sd: 0.37)** **t(19)=-3.51** **p=0.0023**	-0.362 (sd: 0.27) t(19)=-2.98 p=0.0077	**-0.549 (sd: 0.16)** **t(19)=-7.81** **p<0.00001**	0.016 (sd: 0.24) t(19)=0.15 p=0.8814
#2	8ms	-0.164 (sd: 0.27) t(14)=-1.39 p=0.19	**-0.408 (sd: 0.18)** **t(14)=-5.02** **p=0.0002**	-0.035 (sd: 0.13) t(14)=-0.6 p=0.57	0.002 (sd: 0.09) t(14)=0.05 p=0.96	-0.084 (sd: 0.2) t(14)=-0.93 p=0.37
#3	4ms	**0.421 (sd: 0.26)** **t(14)=3.59** **p=0.003**	0.142 (sd: 0.12) t(14)=2.68 p=0.018	0.062 (sd: 0.14) t(14)=0.96 p=0.35		
	8ms	0.193 (sd: 0.19) t(14)=2.32 p=0.03	-0.01 (sd: 0.11) t(14)=-0.2 p=0.84	0.015 (sd: 0.08) t(14)=0.44 p=0.66		
	12ms	**-0.172 (sd: 0.06)** **t(14)=-6.26** **p<0.00001**	**-0.115 (sd: 0.07)** **t(14)=-3.77** **p=0.002**	-0.104 (sd: 0.09) t(14)=-2.57 p=0.02		
	16ms	0.077 (sd: 0.24) t(14)=0.72 p=0.48	-0.087 (sd: 0.09) t(14)=-2.13 p=0.05	-0.023 (sd: 0.13) t(14)=-0.41 p=0.69		
#4	4ms	-0.732 (sd: 0.56) t(14)=-2.53 p=0.02	-0.56 (sd: 0.44) t(14)=-2.45 p=0.028	-0.747 (sd: 0.5) t(14)=-2.88 p=0.01	-0.407 (sd: 0.56) t(14)=-1.41 p=0.18	
	8ms	-0.85 (sd: 0.53) t(14)=-3.12 p=0.008	-0.653 (sd: 0.53) t(14)=-2.38 p=0.032	-0.556 (sd: 0.57) t(14)=-1.9 p=0.078	**-1.762 (sd: 0.3)** **t(14)=-11.33** **p<0.00001**	
	12ms	-0.744 (sd: 0.6) t(14)=-2.4 p=0.03	-0.92 (sd: 0.46) t(14)=-3.88 p=0.002	0.09 (sd: 0.49) t(14)=0.36 p=0.73	**-1.821 (sd: 0.31)** **t(14)=-11.27** **p<0.00001**	
	16ms	-1.001 (sd: 0.63) t(14)=-3.09 p=0.008	**-1.093 (sd: 0.49)** **t(14)=-4.36** **p=0.0007**	-0.334 (sd: 0.54) t(14)=-1.21 p=0.25	**-1.529 (sd: 0.38)** **t(14)=-7.81** **p<0.00001**	
#5	4ms	-0.201 (sd: 0.23) t(19)=-1.92 p=0.069	-0.313 (sd: 0.21) t(19)=-3.29 p=0.0038	-0.2 (sd: 0.18) t(19)=-2.43 p=0.02	-0.269 (sd: 0.26) t(19)=-2.34 p=0.03	

	8ms	-0.251 (sd: 0.6) t(19)=-0.93 p=0.36	-0.087 (sd: 0.23) t(19)=-0.83 p=0.41	-0.07 (sd: 0.15) t(19)=-1.02 p=0.32	**-0.783 (sd: 0.23)** **t(19)=-7.75** **p<0.00001**	
	12ms	-0.173 (sd: 0.27) t(19)=-1.43 p=0.16	0.023 (sd: 0.11) t(19)=0.47 p=0.65	-0.076 (sd: 0.17) t(19)=-1.01 p=0.33	**-0.696 (sd: 0.25)** **t(19)=-6.23** **p<0.00001**	
	16ms	-0.403 (sd: 0.48) t(19)=-1.88 p=0.07	-0.018 (sd: 0.19) t(19)=-0.21 p=0.83	-0.276 (sd: 0.25) t(19)=-2.51 p=0.022	**-0.874 (sd: 0.14)** **t(19)=-13.62** **p<0.00001**	
#6	8ms	**-0.291 (sd: 0.18)** **t(12)=-3.59** **p=0.004**	-0.362 (sd: 0.24) t(12)=-3.36 p=0.006	-0.027 (sd: 0.32) t(12)=-0.19 p=0.86	0.016 (sd: 0.21) t(12)=0.17 p=0.87	
	12ms	-0.018 (sd: 0.2) t(12)=-0.2 p=0.84	**-0.343 (sd: 0.2)** **t(12)=-3.79** **p=0.0026**	0.086 (sd: 0.19) t(12)=1.02 p=0.33	0.026 (sd: 0.05) t(12)=1.13 p=0.29	
	16ms	-0.054 (sd: 0.13) t(12)=-0.93 p=0.37	-0.093 (sd: 0.32) t(12)=-0.65 p=0.53	0.104 (sd: 0.16) t(12)=1.48 p=0.17	-0.019 (sd: 0.08) t(12)=-0.52 p=0.61	
#7	4ms	-0.02 (sd: 0.18) t(15)=-0.25 p=0.80	0.049 (sd: 0.17) t(15)=0.65 p=0.52	**-0.388 (sd: 0.23)** **t(15)=-3.71** **p=0.002**	-0.015 (sd: 0.18) t(15)=-0.19 p=0.85	
	8ms	0.113 (sd: 0.16) t(15)=1.55 p=0.14	-0.081 (sd: 0.13) t(15)=-1.36 p=0.20	-0.488 (sd: 0.32) t(15)=-3.42 p=0.004	**-0.309 (sd: 0.17)** **t(15)=-4.1** **p=0.0009**	
	16ms	-0.132 (sd: 0.19) t(15)=-1.55 p=0.14	-0.203 (sd: 0.19) t(15)=-2.44 p=0.03	-0.209 (sd: 0.2) t(15)=-2.39 p=0.030	-0.111 (sd: 0.23) t(15)=-1.1 p=0.29	
#8	4ms	-0.051 (sd: 0.1) t(14)=-1.16 p=0.27	**0.573 (sd: 0.22)** **t(14)=5.72** **p=0.0001**	0.027 (sd: 0.18) t(14)=0.34 p=0.74	0.141 (sd: 0.21) t(14)=1.47 p=0.16	-0.027 (sd: 0.08) t(14)=-0.74 p=0.48
	8ms	-0.043 (sd: 0.23) t(14)=-0.43 p=0.67	-0.039 (sd: 0.14) t(14)=-0.65 p=0.53	0.188 (sd: 0.12) t(14)=3.37 p=0.004	0.076 (sd: 0.16) t(14)=1.05 p=0.31	0.165 (sd: 0.18) t(14)=2.05 p=0.06
	12ms	-0.022 (sd: 0.09) t(14)=-0.54 p=0.60	0.016 (sd: 0.15) t(14)=0.23 p=0.82	0.007 (sd: 0.26) t(14)=0.06 p=0.95	**0.16 (sd: 0.08)** **t(14)=4.49** **p=0.0005**	0.084 (sd: 0.07) t(14)=2.54 p=0.02
	16ms	-0.012 (sd: 0.17) t(14)=-0.15 p=0.88	-0.099 (sd: 0.14) t(14)=-1.6 p=0.13	0.046 (sd: 0.04) t(14)=2.93 p=0.012	**0.285 (sd: 0.15)** **t(14)=4.21** **p=0.0009**	-0.026 (sd: 0.1) t(14)=-0.57 p=0.58
#9	4ms	-0.018 (sd: 0.1) t(22)=-0.39 p=0.70	-0.042 (sd: 0.2) t(22)=-0.46 p=0.65	-0.014 (sd: 0.07) t(22)=-0.47 p=0.65		
	8ms	-0.006 (sd: 0.14) t(22)=-0.09 p=0.93	0.059 (sd: 0.18) t(22)=0.72 p=0.48	**1.208 (sd: 0.13)** **t(22)=20.46** **p<0.00001**		
	12ms	0.026 (sd: 0.22) t(22)=0.26 p=0.7932	-0.026 (sd: 0.17) t(22)=-0.34 p=0.73	**0.558 (sd: 0.19)** **t(22)=6.62** **p<0.00001**		

	16ms	-0.057 (sd: 0.13) t(22)=-0.95 p=0.35	-0.023 (sd: 0.17) t(22)=-0.3 p=0.77	**0.845 (sd: 0.14)** **t(22)=13.17** **p<0.00001**		
#10	8ms	-0.116 (sd: 0.18) t(13)=-1.46 p=0.1676	0.016 (sd: 0.11) t(13)=0.33 p=0.7491	-0.007 (sd: 0.09) t(13)=-0.17 p=0.8681	-**0.312 (sd: 0.22)** **t(13)=-3.17** **p=0.0075**	**0.387 (sd: 0.21)** **t(13)=4.12** **p=0.0012**
#11	8ms	**0.885 (sd: 0.17)** **t(13)=11.58** **p<0.00001**	**0.871 (sd: 0.1)** **t(13)=19.65** **p<0.00001**	-0.085 (sd: 0.15) t(13)=-1.3 p=0.22	-0.091 (sd: 0.11) t(13)=-1.87 p=0.084	**0.74 (sd: 0.27)** **t(13)=6.09** **p<0.00001**
#12	8ms	-0.131 (sd: 0.44) t(15)=-0.67 p=0.51	-0.231 (sd: 0.72) t(15)=-0.72 p=0.49	**0.715 (sd: 0.24)** **t(15)=6.81** **p<0.00001**	0.058 (sd: 0.35) t(15)=0.37 p=0.71	
	12ms	0.041 (sd: 0.38) t(15)=0.24 p=0.81	0.122 (sd: 0.53) t(15)=0.52 p=0.61	**0.791 (sd: 0.14)** **t(15)=12.91** **p<0.00001**	-0.343 (sd: 0.47) t(15)=-1.64 p=0.12	
	16ms	-0.167 (sd: 0.52) t(15)=-0.72 p=0.48	0.03 (sd: 0.18) t(15)=0.37 p=0.71	0.288 (sd: 0.25) t(15)=2.56 p=0.02	-0.288 (sd: 0.34) t(15)=-1.9 p=0.08	
#13	8ms	-0.174 (sd: 0.2) t(14)=-1.92 p=0.07	-0.211 (sd: 0.19) t(14)=-2.46 p=0.03	**0.833 (sd: 0.21)** **t(14)=8.93** **p<0.00001**		
	12ms	-0.005 (sd: 0.18) t(14)=-0.06 p=0.95	**0.441 (sd: 0.09)** **t(14)=10.64** **p<0.00001**	**1.044 (sd: 0.17)** **t(14)=14.06** **p<0.00001**		
	16ms	-0.093 (sd: 0.16) t(14)=-1.29 p=0.22	**0.274 (sd: 0.14)** **t(14)=4.54** **p=0.0005**	**1.242 (sd: 0.16)** **t(14)=17.91** **p<0.00001**		
#14	8ms	-0.039 (sd: 0.11) t(13)=-0.81 p=0.43	-0.068 (sd: 0.12) t(13)=-1.29 p=0.22	-0.015 (sd: 0.09) t(13)=-0.37 p=0.72	-0.034 (sd: 0.11) t(13)=-0.7 p=0.49	-0.032 (sd: 0.08) t(13)=-0.91 p=0.38
	12ms	-0.009 (sd: 0.1) t(13)=-0.2 p=0.85	-0.061 (sd: 0.11) t(13)=-1.24 p=0.24	0.004 (sd: 0.11) t(13)=0.08 p=0.94	-0.023 (sd: 0.1) t(13)=-0.53 p=0.61	-0.035 (sd: 0.09) t(13)=-0.87 p=0.40
	16ms	-0.043 (sd: 0.12) t(-1)=-0.81 p=0.43	-0.036 (sd: 0.11) t(13)=-0.73 p=0.48	-0.032 (sd: 0.12) t(13)=-0.6 p=0.56	0.02 (sd: 0.12) t(13)=0.39 p=0.71	0.046 (sd: 0.12) t(13)=0.87 p=0.40
#15	8ms	-0.026 (sd: 0.12) t(13)=-0.48 p=0.64	0.037 (sd: 0.13) t(13)=0.63 p=0.54	-0.021 (sd: 0.11) t(13)=-0.43 p=0.67	-0.043 (sd: 0.09) t(13)=-1.12 p=0.28	-0.061 (sd: 0.08) t(13)=-1.74 p=0.11
	12ms	-0.091 (sd: 0.1) t(13)=-2.07 p=0.06	-0.049 (sd: 0.1) t(13)=-1.06 p=0.31	-0.077 (sd: 0.09) t(13)=-1.86 p=0.09	-0.091 (sd: 0.11) t(13)=-1.85 p=0.08	-0.089 (sd: 0.15) t(13)=-1.37 p=0.20
	16ms	-0.021 (sd: 0.13) t(-1)=-0.37 p=0.72	-0.038 (sd: 0.14) t(13)=-0.59 p=0.56	-0.09 (sd: 0.09) t(13)=-2.13 p=0.05	0.015 (sd: 0.1) t(13)=0.35 p=0.72	0.008 (sd: 0.12) t(13)=0.15 p=0.89
#16	8ms	0.071 (sd: 0.18) t(17)=0.9 p=0.38	0.13 (sd: 0.16) t(17)=1.88 p=0.07	0.038 (sd: 0.15) t(17)=0.57 p=0.58	0.005 (sd: 0.12) t(17)=0.1 p=0.93	0.084 (sd: 0.2) t(17)=0.94 p=0.36

	12ms	-0.018 (sd: 0.16) t(17)=-0.26 p=0.80	0.065 (sd: 0.18) t(17)=0.82 p=0.42	-0.022 (sd: 0.2) t(17)=-0.25 p=0.80	-0.013 (sd: 0.2) t(17)=-0.15 p=0.88	0.01 (sd: 0.21) t(17)=0.11 p=0.91
	16ms	-0.034 (sd: 0.15) t(-1)=-0.51 p=0.61	0.013 (sd: 0.19) t(17)=0.15 p=0.88	-0.044 (sd: 0.2) t(17)=-0.49 p=0.63	0.021 (sd: 0.17) t(17)=0.28 p=0.78	-0.017 (sd: 0.18) t(17)=-0.22 p=0.83
#17	4ms	-0.066 (sd: 0.36) t(13)=-0.42 p=0.68	-0.116 (sd: 0.41) t(13)=-0.64 p=0.53	0.118 (sd: 0.27) t(13)=0.97 p=0.35	-0.205 (sd: 0.34) t(13)=-1.37 p=0.19	0.002 (sd: 0.22) t(13)=0.02 p=0.98
	8ms	-0.189 (sd: 0.36) t(13)=-1.18 p=0.26	-0.022 (sd: 0.24) t(13)=-0.2 p=0.85	-0.074 (sd: 0.39) t(13)=-0.43 p=0.67	0.106 (sd: 0.2) t(13)=1.18 p=0.26	-0.302 (sd: 0.42) t(13)=-1.61 p=0.13
	16ms	-0.173 (sd: 0.38) t(13)=-1.03 p=0.32	0.174 (sd: 0.31) t(13)=1.28 p=0.22	-0.04 (sd: 0.29) t(13)=-0.3 p=0.77	-0.163 (sd: 0.31) t(13)=-1.18 p=0.26	0.026 (sd: 0.31) t(13)=0.19 p=0.85

Table 2: statistics on individual patients, for each conditioning electrode and each ISI. *The data reported correspond to the log of the ratio between conditioned MEPs and test MEPs. The table reports the mean value (standard deviation), and the t-statistics of the single-sample t-tests: t-value (degrees of freedom) and p-value. Please note that the log-ratio has no dimensions because it is obtained by dividing two identical dimensions. Note also that degrees of freedom are variable according to the number of single trials that were performed in that particular condition. Conditions with p-values exceeding the Bonferroni-corrected significance threshold are highlighted in bold. A corresponding graphical representation of the data is provided in Figure 4.*